Phys. Status Solidi A **207**, No. 7, 1735–1740 (2010) / **DOI** 10.1002/pssa.200983706

physica status solidi a
www.pss-a.com
applications and materials science

Ultraviolet photoconductive sensor based on single ZnO nanowire

O. Lupan[*,1,2], G. Chai[3], L. Chow[,1,4], G. A. Emelchenko[5], H. Heinrich[1,4], V. V. Ursaki[6,7], A. N. Gruzintsev[8], I. M. Tiginyanu[7,9], and A. N. Redkin[8]**

[1] Department of Physics, University of Central Florida, PO Box 162385, Orlando, FL 32816, USA
[2] Department of Microelectronics and Semiconductor Devices, Technical University of Moldova, Stefan cel Mare Blvd. 168, 2004 Chisinau, Republic of Moldova
[3] Apollo Technologies, Inc. 205 Waymont Court, S111, Lake Mary, FL 32746, USA
[4] Advanced Materials Processing and Analysis Center, and Department of Mechanical, Materials, and Aerospace Engineering, University of Central Florida, PO Box 162385, Orlando, FL 32816, USA
[5] Institute of Solid State Physics, Russian Academy of Science, 142432 Chernogolovka, Moscow District, Russia
[6] Institute of Applied Physics of the Academy of Sciences of Moldova, 2028 Chisinau, Republic of Moldova
[7] National Center for Materials Study and Testing, Technical University of Moldova, 2004 Chisinau, Republic of Moldova
[8] Institute of Microelectronics Technology and High Purity Materials, Russian Academy of Sciences, 142432 Chernogolovka, Moscow District, Russia
[9] Laboratory of Nanotechnology, Institute of Electronic Engineering and Industrial Technologies, Academy of Sciences of Moldova, 2028 Chisinau, Republic of Moldova

Received 30 May 2009, revised 24 October 2009, accepted 15 January 2010
Published online 28 May 2010

Keywords CVD, nanodevices, nanowires, photoconduction, structure, ZnO

* Corresponding author: e-mail lupan@physics.ucf.edu, lupanoleg@yahoo.com, Phone: +1 407 823 5117, Fax: +1 407 823 5112
** e-mail chow@mail.ucf.edu, Phone: +1 407 823 2333, Fax: +1 407 823 5112

ZnO nanowires were synthesized by the CVD procedure and have been investigated by SEM, TEM, SAED, Raman, and cw PL spectroscopy. The fabrication of an ultraviolet (UV) photoconductive detector based on single ZnO nanowire (100 nm in diameter) is presented. This nanostructure detector is prepared in an Focused Ion Beam (FIB) set-up by using nanodeposition for metal electrodes. The photoresponse of the UV sensor are studied using a UV source with an incident peak wavelength of 365 nm. It was demonstrated that the output signal of the sensors is reproducible under UV irradiation. The photoresponse and characteristics of the ZnO nanowire-device demonstrates that focused ion beam process offers a way to fabricate novel nanodevices on a single ZnO nanowire with diameters as small as 100 nm. The presented single ZnO nanowire sensor proves to be promising for application in various processes.

1 Introduction Recently, wide-gap semiconducting oxide micro- and nanostructures based on ZnO, SnO_2, TiO_2 have attracted tremendous research interest due to their ultraviolet (UV) photoresponse and their optical transparency in the visible spectral range [1–9]. In particular, quasi-one-dimensional (Q1D) ZnO nanowires/nanorods are promising as a new type of low-cost and high-speed UV nanoscale photoconductive detectors and optical switches [1, 2, 6, 7, 9]. The low dimensions of such nanostructures promise increase in electronic device packing density, low power consumption, and also enhanced UV sensing properties. Q1D nanostructures with small diameters (<100 nm) exhibit a large surface-to-volume ratio which makes them highly susceptible to altered electrical properties by means of electron–hole generation or recombination during UV exposure.

UV detection with nanowires is normally realized by monitoring the current–voltage or the electrical conductance variation when exposed to UV radiation. Due to the unique geometry of nanowires the active volume contributing to dark current (as a source of noise) is one thousandth of a normal size detector. This allows one to reach a higher sensitivity by using a single nanowire in devices.

In particular, Yang and co-workers [1] used electron-beam lithography to fabricate nanowire-based UV

photodetectors and optical switches. Harnack et al. [10] studied photoresponse to 366 nm UV light of the ZnO nanorods electrically aligned between interdigitated gold electrodes on SiO_2. Suehiro et al. [11] reported dielectrophoretic fabrication of an individual ZnO nanowire based UV sensor with a relatively slow response, but a high UV sensitivity of 10 nW cm^{-2}. Law and Thong [12] fabricated a ZnO nanowire UV photodetector with a photoresponse time of 0.4 ms by growing it between two patterned zinc electrodes. It is known that the UV photoresponse of ZnO can be affected by nanostructure size, aspect ratio, crystallographic orientation, Zn^- or O^- terminated surface, surface defects, and post-annealing [13–15]. So far, a large number of techniques have been exploited to fabricate ZnO nanostructures/nanowires [16–18] and photodetectors [1, 7, 9–10].

The goal of this paper is to demonstrate that chemical vapor deposition (CVD) can be used for the preparation of transferable ZnO nanowires with high crystallinity, good optical properties, and sensitivity to UV radiation, which allows one to construct nanoscale photodetectors by using a FIB instrument.

2 Experimental The ZnO nanowires were synthesized by the CVD procedure on a Si(100) substrate. Metallic zinc of high purity (99.999%) and an oxygen–argon mixture (20 vol.% oxygen) were used as starting reactants [19]. The synthesis was performed in a flowing type two-zone quartz reactor. In the first zone zinc evaporated, while in the second zone zinc vapors interacted with oxygen. Substrates of (100)-oriented silicon wafers were placed in the second zone. The temperature of zinc source evaporation was 670 °C, the growth temperature was 650 °C (2nd zone). The oxygen–argon mixture was fed to the reactor at a rate of 1 l/h. The synthesis was conducted for 30 min.

The morphology of the samples was studied by a scanning electron microscope (SEM, Hitachi, operating at 10 kV) equipped with an EDX spectroscope. The EDX spectroscope was used to explore the ZnO chemical composition (within a precision of 1 at.%).

The crystalline quality of ZnO nanowires were analyzed by X-ray diffraction (XRD). The structural characterization of a single nanowire was performed by high-resolution transmission electron microscopy (HRTEM) with a FEI Tecnai F-30 microscope operating at 300 kV.

The continuous wave (cw) photoluminescence (PL) was excited by the 351.1 nm line of a Spectra-Physics Ar^+ laser and analyzed with a double spectrometer ensuring a spectral resolution better than 0.5 meV. The samples were mounted on the cold station of a LTS-22-C-330 optical cryogenic system. The Raman scattering was investigated at room temperature with a MonoVista CRS Confocal Laser Raman System in the backscattering geometry under the excitation by a 532 nm DPSS laser.

The focused ion beam (FIB) was employed for the photodetector fabrication. The UV sensitivity was measured using a two-terminal ZnO nanowire device excited by the 365 nm line of an Hg-lamp.

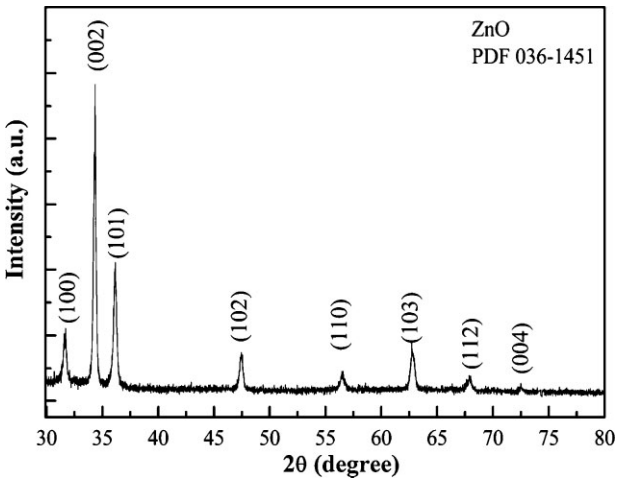

Figure 1 XRD spectrum for ZnO nanowires grown by CVD on a Si substrate.

3 Results and discussions

3.1 Structural characterization Figure 1 presents an indexed XRD scan in the range of 30–80° on the ZnO nanowires grown by CVD. One can see that all the diffraction peaks correspond to crystalline ZnO with the hexagonal wurtzite structure [20]. The calculated lattice constant $c = 0.522$ nm is consistent with the standard values. No characteristic peaks from other impurities are detected. In Fig. 1, the strongest detected (*hkl*) peak is at 2θ values of 34.4°, corresponding to the lattice plane (002) in ZnO. It also was detected lower intensity ZnO peaks at 31.7, 36.2, 47.5, 56.6, 62.7, and 72.6° corresponding to the following lattice planes: (100), (101), (102), (110), (103), (004), respectively.

3.2 Morphological characterization A typical SEM image taken from ZnO nanowires grown by CVD is shown in Fig. 2. The ZnO nanowires have an average radius of 50 nm and the mean length is about 5 μm.

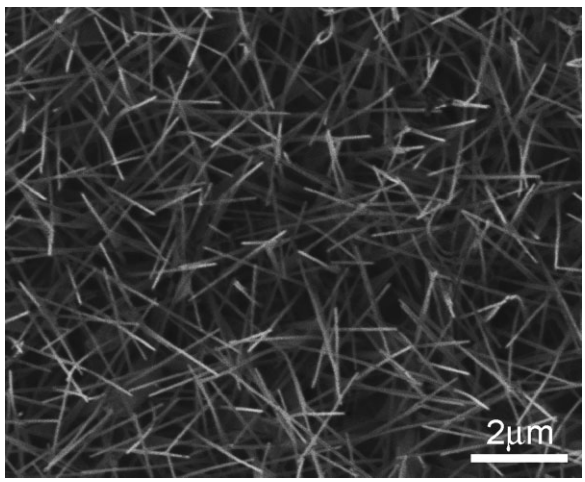

Figure 2 SEM image taken from ZnO nanowires grown on Si substrate by CVD process at 650 °C.

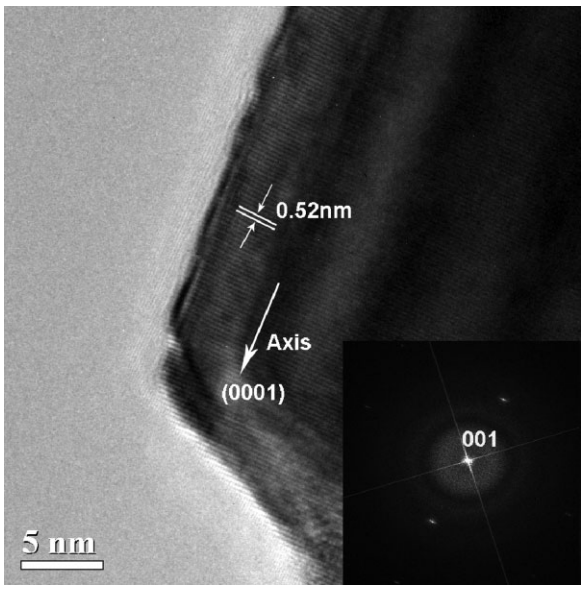

Figure 3 TEM image taken from a side edge of CVD synthesized ZnO nanowire and a typical SAED pattern (see inset).

According to our experimental results, the nanowires obtained by CVD process can be transferred to other substrates and can be handled by a Focused Ion Beam (FIB) instrument in order to fabricate test devices.

A TEM image and a selective-area electron diffraction (SAED) pattern of an individual ZnO nanowire are shown in Fig. 3. The lattice fringes in all examined regions reveal no dislocations or stacking faults, illustrating that the nanowire consists of a defect-free single crystal. The TEM analysis (Fig. 3) demonstrates that single crystalline ZnO nanowires grow along the [0001] axis.

The HRTEM image displays clearly resolved lattice distances of 0.52 nm along the long axis of a nanowire coinciding with the (0001) lattice spacing. A SAED pattern (inset in Fig. 3) taken from a ZnO nanowire showed both single crystalline nature of distinct diffraction spots plus nanocrystalline nature of diffusive diffraction rings. The [001] crystallographic direction shown in the inset indicated the preferential growth direction of the ZnO.

3.3 Optical properties The cw PL characterization revealed the high optical quality of the ZnO structures. The spectrum is dominated by the donor excitonic (DX) emission, while the emission related to the donor acceptor pair recombination DA is two orders of magnitude less intensive. Apart from the high intensity of the emission related to the recombination of neutral donor bound excitons D^0X, the high optical quality of the nanowires is indicated by well resolved I_1, I_4, and I_6 lines related to different donors [21] and the presence of the emission related to the recombination of free excitons FX. The other PL bands observed in the spectra are associated with the phonon replica of the neutral donor bound excitons D^0X and donor acceptor pair recombination DA PL lines (Fig. 4).

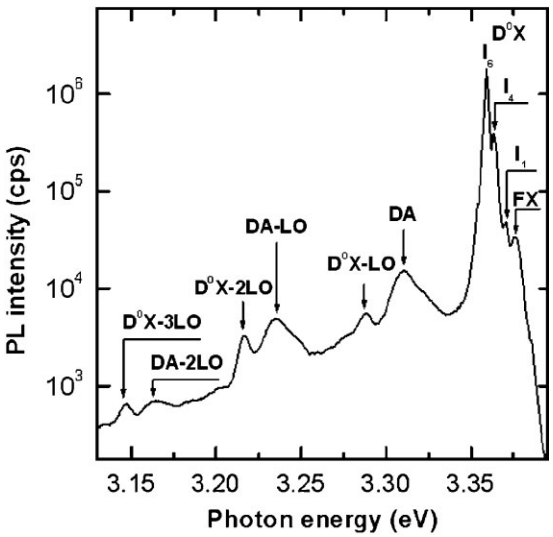

Figure 4 PL spectrum of the ZnO nanowires grown by CVD process and measured at $T = 10$ K.

The exploration of vibrational properties of ZnO nanowires is important for shedding light upon the transport properties and phonon interaction with the free carriers, which determine the optoelectronic device performance [22]. It was demonstrated that carriers excited high in the conduction band relax toward their ground state mainly by Fröhlich interaction with the longitudinal optical phonons. The dynamics of the phonon population strongly affects the performance of optoelectronic devices [23].

The room-temperature Raman scattering spectrum of the ZnO nanowires is illustrated in Fig. 5. This spectrum demonstrates the good crystalline quality of the wurtzite crystal structure in the produced material. Wurtzite ZnO belongs to the C_{6v}^4 space group ($P6_3mc$). The primitive cell includes two formula units with all atoms occupying 6b sites of symmetry C_{3v}. According to group theory, the corresponding zone centre optical phonons are of the following

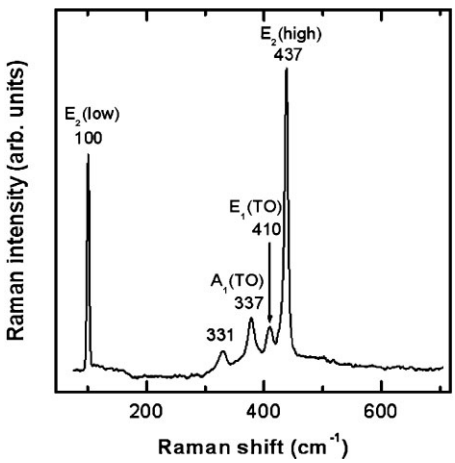

Figure 5 Micro-Raman spectrum of ZnO nanowires measured at room temperature.

symmetry modes: $A_1 + 2B_1 + E_1 + 2E_2$ [24]. The A_1, E_1, and $2E_2$ are the first-order Raman active modes, while $2B_1$ phonons are silent.

The A_1 and E_1 modes are also infrared-active and therefore split into longitudinal LO and transverse TO optical components. Except for the LO modes, all Raman active phonon modes are clearly identified in the measured spectrum (Fig. 5). The peaks at 100 and 437 cm^{-1} are attributed to ZnO nonpolar optical phonon E_2(low) and E_2(high) modes, respectively. The peak at 410 cm^{-1} corresponds to the E_1(TO) mode. The peak at 331 cm^{-1} is attributed to second order Raman processes involving acoustic phonons [25]. There are several indicatives of a good crystal quality of the produced nanostructures: (i) the signal attributed to the two-phonon density of states (DOS) expected in the spectral range from 500 to 700 cm^{-1} [26, 27] is practically absent in the sample; (ii) the peak corresponding to E_2(high) mode has a linewidth of about 6 cm^{-1}, while the linewidth of the peak corresponding to E_2(low) mode is about 3 cm^{-1}, which is comparable to values reported for high quality ZnO bulk crystals [28]; (iii) the position of the E_2 (high) peak corresponds to the phonon of a bulk ZnO crystal [28] indicating a strain-free state of the nanowire.

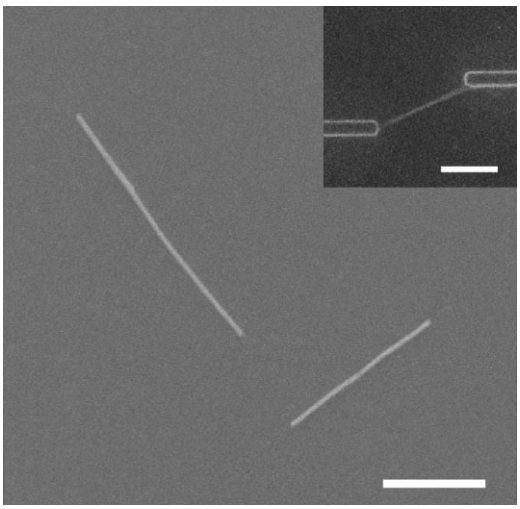

Figure 6 Secondary electron micrographs showing the transferred ZnO nanowires on a substrate for fabrication procedure in the FIB system. Inset shows a single ZnO nanowire welded to two electrode/external connections as final photoconductive nanodetector. The scale bar is 2 μm.

3.4 Nanofabrication of a sensor based on single ZnO nanowire A FIB system was used for fabrication of a UV photoconductive sensor. A micromanipulator was mounted beside the stage in the FIB instrument and was used for sample manipulation and lift-out process [30–32]. A glass substrate with predeposited Au/Cr electrodes was used as a template with external electrodes/connections. The ZnO nanowire was transferred from the initial Si substrate to the Au/Cr patterned substrate by sonication to disperse isolated nanowires on second substrate with preformed electrodes.

We also used a direct contact technique to transfer nanowires by direct contact of the sample with a clean Si/SiO_2 wafer prepared according to [29–32] and gently rub a few times. These procedures allow us to obtain a low density and uniformly distributed ZnO nanowires on the second substrate. If one needs to lower the density of NWs, the above procedure can be repeated [30, 31]. Pt lines with dimensions of 0.5 μm × 0.5 μm × 5 μm connected to one of the Au/Cr external contacts were used to avoid charging problems during the fabrication process. Then we scan the surface of the substrate for a conveniently oriented ZnO nanowire (Fig. 6). Afterwards, focused ion beam is used to deposit Pt conducting lines to connect the ZnO nanowire with the pre-deposited Cr/Au contact electrodes on the substrate. Inset in Fig. 6 shows a single ZnO nanowire-based photodetector fabricated in the FIB system.

3.5 UV sensing properties The room temperature sensitivity of the single nanowire ZnO nanophotodetector to 365 nm UV light is shown in Fig. 7. When the ZnO nanowire photodetector is illuminated by 365 nm UV light, the electrical resistance decreases with a time constant of 2 min (as shown in Fig. 7). When the UV light is turned off the resistance increases back to within 10% of the initial value with a recovery time of 3 min. Multiple experiments were performed and similar results were obtained with an accuracy of 7–10% for time constants.

The UV response and recovery times are relatively fast for a single ZnO nanowire photodetector comparing to an individual zinc oxide nanorod grown by aqueous chemical deposition [3]. The measured resistance change of about 12% for single CVD ZnO nanowire is several times higher than reported previously [3, 7].

The photodetection mechanism can be proposed as follows. Initially, oxygen molecules adsorbed on the surface

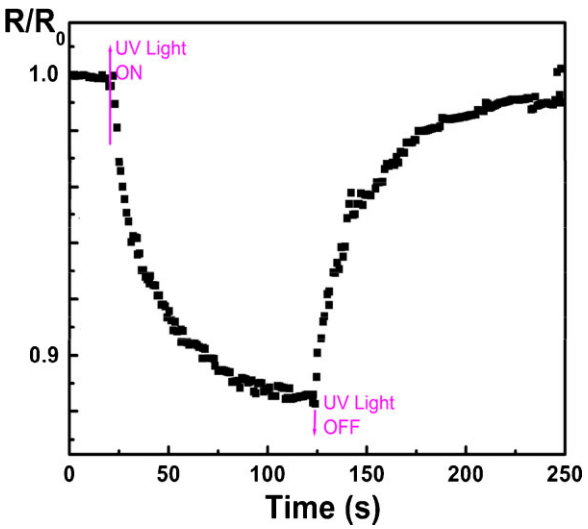

Figure 7 (online color at: www.pss-a.com) The UV response for a single ZnO nanowire-based UV photoconductive sensor.

of ZnO nanowire decrease the carriers' density by trapping free electrons ($O_2(g) + e^- \rightarrow O_2^-(ad)$). This leads to the formation of a depletion region near the surface which significantly decreases the conductance. The UV response time is governed by adsorption and desorption of O_2 molecules on the surface [2, 3, 7, 30]. After the photosensor is illuminated by UV light, the electron–hole (e^-–h^+) pairs will be generated ($h\nu \rightarrow e^- + h^+$). The holes ($h^+$) will migrate to the surface to discharge the chemisorbed oxygen ions and lowering the depletion layer near the surface ($O_2^-(ad) + h^+ \rightarrow O_2(g)$). The remaining unpaired electrons will contribute to the current. After UV light is turned off, the holes concentration is lower than that of electrons in the ZnO nanowire. However, h^+ recombines with e^-, simultaneously oxygen molecules readsorb on the surface and capture free electrons. This will result in a decrease of the conductance value. Several photodetectors have been fabricated by the presented technique and have been investigated under identical conditions. The levels of UV responses were found to be very close to each other. The obtained results demonstrate the feasibility of the single nanowire-based device structures for detecting UV light.

4 Conclusions In conclusion, the ZnO nanowires were synthesized by the CVD procedure with an average radius of 50 nm and the mean length is about 5 μm. TEM and a SAED results from an individual ZnO nanowire reveal no dislocations and a defect-free single crystal. The cw PL demonstrates the high optical quality of the ZnO structures and the spectrum is dominated by the DX emission. From the Raman studies can be concluded several indicatives of a good crystal quality of the produced nanostructures: (1) the signal attributed to the two-phonon DOS expected in the spectral range from 500 to 700 cm^{-1} is practically absent in the sample; (2) the peak corresponding to E_2(high) and E_2(low) modes are comparable to values reported for high quality ZnO crystals [28]; (3) the position of the E_2 (high) peak corresponds to the phonon of a bulk ZnO crystal [28].

We have fabricated a UV photoconductive sensor based on single ZnO nanowire grown by CVD with a diameter as low as 100 nm. Focused ion beam FIB instrument is used in the fabrication process. The UV response and recovery times (of ~2 min) of CVD ZnO nanowire detector were measured and the feasibility of the individual nanowire–based photodetectors was demonstrated. A sensing mechanism is discussed based on the observed experimental results.

Acknowledgements L. Chow acknowledges partial financial support from Apollo Technologies, Inc. and Florida High Tech Corridor Program. Financial support by the Russian Foundation for Basic Research (Project no. 08-02-90103) and Supreme Council for Science and Technological Development of the Academy of Sciences of Moldova (Project 036/R) are gratefully acknowledged. Dr. Lupan acknowledges financial support for post-doctoral position in Professor Chow's group.

References

[1] H. Kind, H. Yan, B. Messer, M. Law, and P. Yang, Adv. Mater. **14**, 158 (2002).
[2] C. Soci, A. Zhang, B. Xiang, S. A. Dayeh, D. P. R. Aplin, J. Park, X. Y. Bao, Y. H. Lo, and D. Wang, Nano Lett. **7**, 1003 (2007).
[3] O. Lupan, L. Chow, G. Chai, L. Chernyak, O. Lopatiuk-Tirpak, and H. Heinrich, Phys. Status Solidi A **205**, 2673 (2008).
[4] O. Lupan, L. Chow, G. Chai, A. Schulte, S. Park, and H. Heinrich, Mater. Sci. Eng. B **157**, 101 (2009).
[5] O. Lupan, L. Chow, G. Chai, H. Heinrich, S. Park, and A. Schulte, J. Cryst. Growth **311**, 152 (2008).
[6] L. Chow, O. Lupan, H. Heinrich, and G. Chai, Appl. Phys. Lett. **94**, 163105 (2009).
[7] G. Chai, O. Lupan, L. Chow, and H. Heinrich, Sens. Actuators A **150**, 184 (2009).
[8] R. Martins, E. Fortunato, P. Nunes, I. Ferreira, A. Marques, M. Bender, N. Katsarakis, V. Cimalla, and G. Kiriakidis, J. Appl. Phys. **96**, 1398 (2004).
[9] A. Pimentel, A. Gonçalves, A. Marques, R. Martins, and E. Fortunato, J. Non-Cryst. Solids **352**, 1448 (2006).
[10] O. Harnack, C. Pacholski, H. Weller, A. Yasuda, and J. M. Wessels, Nano Lett. **3**, 1097 (2003).
[11] J. Suehiro, N. Nakagawa, S. Hidaka, M. Ueda, K. Imasaka, M. Higashihata, T. Okada, and M. Hara, Nanotechnology **17**, 2567 (2006).
[12] J. B. K. Law and J. T. L. Thong, Appl. Phys. Lett. **88**, 133114 (2006).
[13] L. Schmidt-Mende and J. L. MacManus-Driscoll, Mater. Today **10**, 40 (2007).
[14] I. L. Lyubchanskii, N. N. Dadoenkova, M. I. Lyubchanskii, E. A. Shapovalov, A. Lakhtakia, and T. Rasing, Appl. Phys. Lett. **85**, 5932 (2004).
[15] Y. Zhang, A. Kolmakov, S. Chretien, H. Metiu, and M. Moskovits, Nano Lett. **4**, 403 (2004).
[16] G. Shen, J. H. Cho, and C. J. Lee, Chem. Phys. Lett. **401**, 414 (2005).
[17] J. Zhang, Y. Yang, B. Xu, F. Jiang, and J. Li, J. Cryst. Growth **280**, 509 (2005).
[18] C. H. Ye, X. S. Fang, Y. F. Hao, X. M. Teng, and L. D. Zhang, J. Phys. Chem. B **109**, 19758 (2005).
[19] A. N. Redkin, Z. I. Makovei, A. N. Gruzintsev, S. V. Dubonos, and E. E. Yakimov, Inorg. Mater. **43**, 253 (2007).
[20] Joint Committee on Powder Diffraction Standards, Powder Diffraction File No. 36-1451.
[21] B. K. Meyer, H. Alves, D. M. Hofmann, W. Kriegseis, D. Forster, F. Bertram, J. Christen, A. Hoffmann, M. Straßburg, M. Dworzak, U. Haboeck, and A. V. Rodina, Phys. Status Solidi B **241**, 231 (2004).
[22] R. Cuscó, E. Alarcón-Lladó, J. Ibáñez, L. Artús, J. Jiménez, B. Wang, and M. J. Callahan, Phys. Rev. B **75**, 165202 (2007).
[23] B. C. Lee, K. W. Kim, M. A. Stroscio, and M. Dutta, Phys. Rev. B **58**, 4860 (1998).
[24] A. Kaschner, U. Haboeck, M. Strassburg, G. Kaczmarczyk, A. Hoffmann, C. Thomsen, A. Zeuner, H. R. Alves, D. M. Hofmann, and B. K. Meyer, Appl. Phys. Lett. **80**, 1909 (2002).
[25] M. Rajalakshmi, A. K. Arora, B. S. Bendre, and S. Mahamuni, J. Appl. Phys. **87**, 2445 (2000).

[26] F. Reuss, C. Kichner, Th. Gruber, R. Kling, S. Maschek, W. Limmer, A. Waag, and P. Ziemann, J. Appl. Phys. **95**, 3385 (2004).
[27] J. Serrano, A. H. Romero, F. J. Manjon, R. Lauck, M. Cardona, and A. Rubio, Phys. Rev. B **69**, 094306 (2004).
[28] J. Serrano, F. J. Manjón, A. H. Romero, F. Widulle, R. Lauck, and M. Cardona, Phys. Rev. Lett. **90**, 055510 (2003).
[29] S. T. Shishiyanu, O. I. Lupan, T. S. Shishiyanu, V. P. Sontea, and S. K. Railean, Electrochim. Acta **49**, 4433 (2004).
[30] O. Lupan, L. Chow, and G. Chai, Sens. Actuators B **141**, 511 (2009).
[31] O. Lupan, V. V. Ursaki, G. Chai, L. Chow, G. A. Emelchenko, I. M. Tiginyanu, A. N. Gruzintsev, and A. N. Redkin, Sens. Actuators B **144**, 56 (2010).
[32] G. Chai, O. Lupan, and L. Chow, Focused ion beam fabrication of carbon nanotube and ZnO nanodevices, in: P. Russell, I. Utke, S. Moshkalev (eds.), Nanofabrication Using Focused Ion and Electron Beams: Principles and Applications, Nanofabrication with FEB and FIB (Oxford University Press, 2010), pp. 1–10.

